

Nanogenerators: a new paradigm in blue energy harvesting

Arpita Adhikari¹ and Joydip Sengupta²

¹*Department of Electronics and Communication Engineering, Techno Main Salt Lake, Kolkata, India*

²*Department of Electronic Science, Jogesh Chandra Chaudhuri College, Kolkata, India*

Chapter Outline

8.1 Introduction	171
8.2 Origin of nanogenerators	172
8.3 Piezoelectric nanogenerator	174
8.4 Triboelectric nanogenerator	176
8.5 Pyroelectric nanogenerator	179
8.6 Thermoelectric nanogenerator	182
8.7 Blue energy harvesting using nanogenerators	184
8.7.1 Water-involved TENG	184
8.7.2 Nonwater-involved TENG	186
8.8 Summary and perspective	188
References	188

8.1 Introduction

The progress of civilization has undoubtedly reached its unprecedented peak with the commencement of the fourth industrial revolution in the 21st century. The present age of industrial advancement quite expectedly is facing an elevated demand for energy resources. Limited storage of natural energy resources is making the situation more critical day by day. Consequently, modern industries are confronting enormous energy challenges. Moreover, the modern time of industrialization threatens the near future of the mankind with the rising level of carbon pollution that paved the path of unpredictable changes of Earth's climate, possibly resulting in even scary extinction of life. The only way-out of the critical situation may be the search for alternative and sustainable energy resources [1]. Within the perspective of climate change, a sustainable energy resource and the utilization need to be pollution-free. Thus the futuristic growth of science and technology is confronting the dual challenge of energy crisis and carbon pollution (Fig. 8.1) [2].

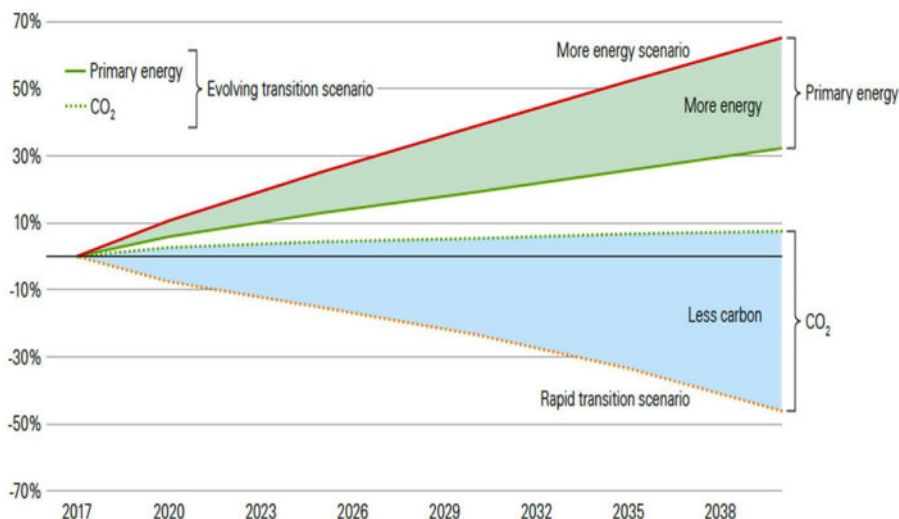


FIGURE 8.1

The global energy system faces a dual challenge: the need for “more energy and less carbon.”

From BP global. <<https://www.bp.com/en/global/corporate.html>>, 2019 (accessed 27.05.20).

8.2 Origin of nanogenerators

The search for alternative energy resources particularly in terms of the nonconventional and sustainable form is the essential prerequisite of the modern society to maintain the futuristic, scientific, technological, and an industrial drive toward a new era of automation. The novel advancement of mankind would not be possible without the revolutionary concept of the Internet of Things (IoT). All of these technological progress are the phenomenal consequences of the technological achievements of miniaturization science. Nanotechnology is the utmost discovery of miniaturization science which even outperformed the projection of technological growth that had been foreseen by Moore, decades before in 1975. The nanotechnology gives birth to nanodevices, which obviously need the power to operate. However, in general, the market-available battery size is much larger than the nanodevices, thus in turn governing the size of the entire system. Consequently, the practical realization of a nanobattery is highly desirable, preferably employing alternative energy resources. The nano-sized battery usually has a small lifetime posing a great hurdle to scientists. The desirable alternative is to develop nanosized battery which can harvest energy from the environment to become a self-sufficient green power resource for driving the nanodevices. Nanogenerators fit within this scope. First, they are of nanosize order, and second, they can convert naturally available mechanical energy into electrical energy. Moreover, this energy suffices to drive the nanodevice in self-power mode. The term nanogenerator was first coined in 1997 [3], while the seed to the invention of nanogenerators was sowed long before in 1861 with the postulation of Maxwell’s equation (Fig. 8.2) [4]. According to Maxwell’s equation, the displacement current has two components. The first term of Maxwell’s equation postulates the origin of magnetic induction from the electric field. The term thus forms the basis of electromagnetic wave generation, the application of

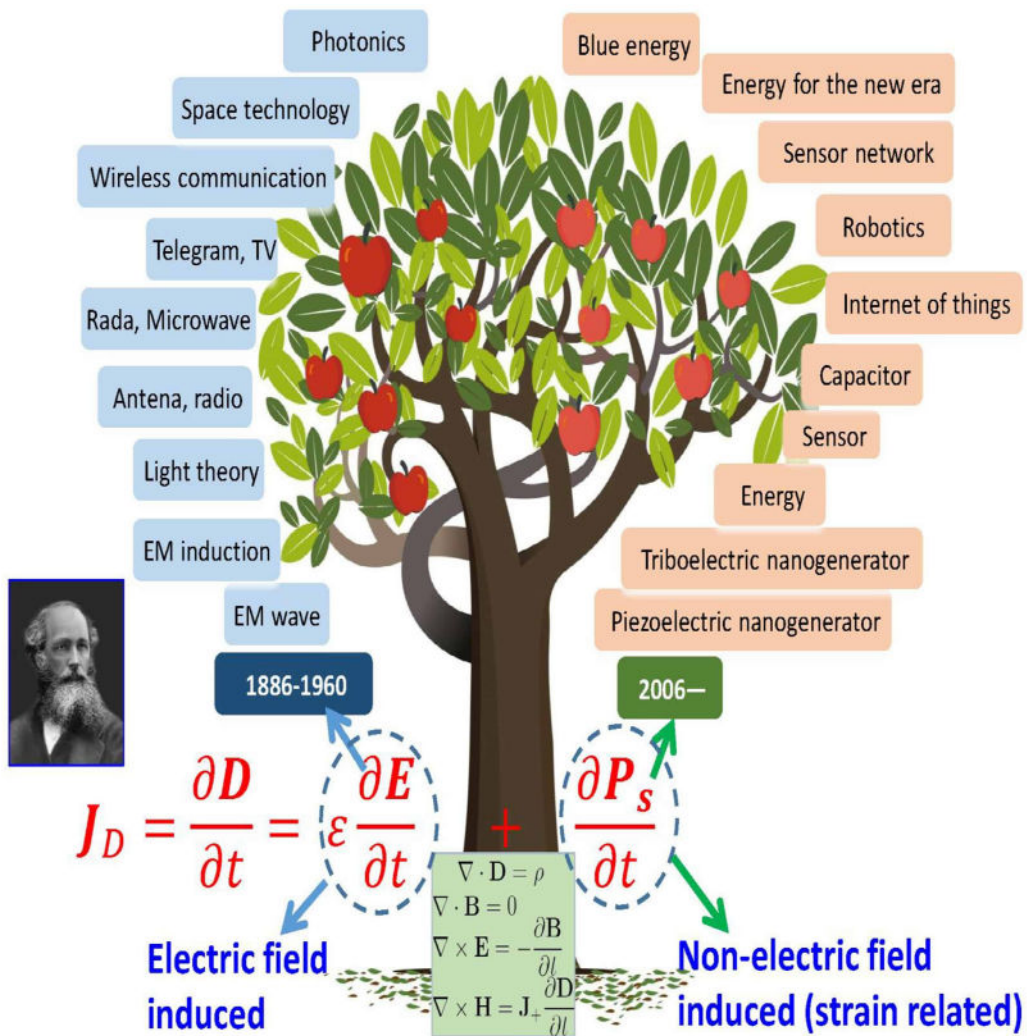
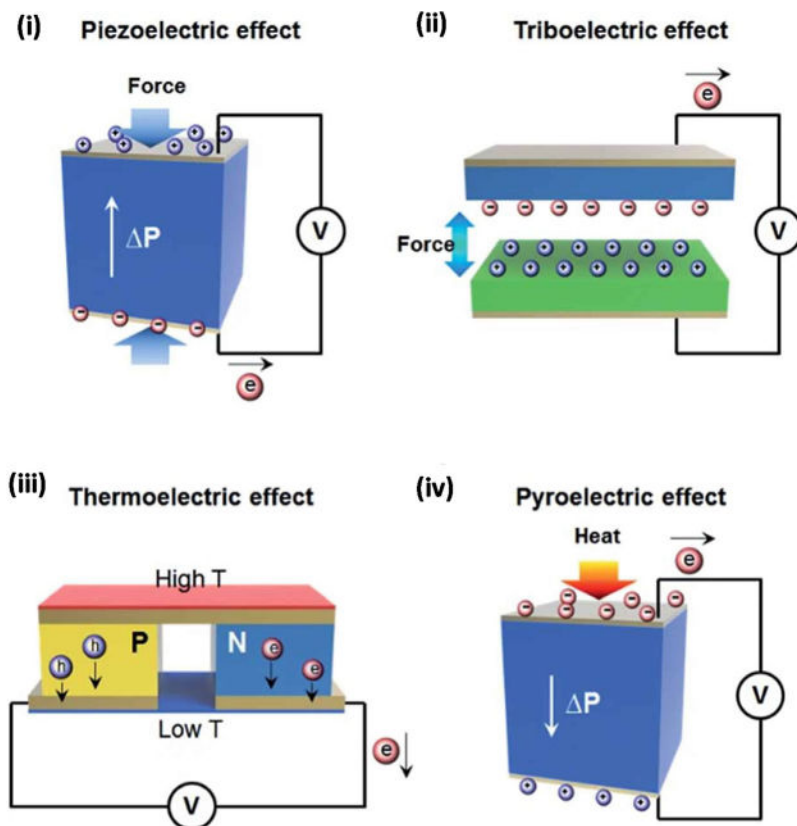


FIGURE 8.2

A tree idea to illustrate the newly revised Maxwell's displacement current: the first term is responsible for the electromagnetic waves theory and the newly added term depicts the applications of Maxwell's equations in energy and sensors, viz., the nanogenerators.

From W.Z. Lin, On the first principle theory of nanogenerators from Maxwell's equations, Nano Energy (2020) 104272.

which extends to modern wireless communication technology. The second term defines the polarization of medium and from which the fundamental features of the nanogenerator originated [5]. In nanogenerators, Maxwell's displacement current serves as the driving force for converting mechanical energy into electrical energy.

**FIGURE 8.3**

Schematic illustration of nanogenerators based on (A) the piezoelectric effect, (B) the triboelectric effect, (C) the thermoelectric effect, and (D) the pyroelectric effect.

From L. Ju-Hyuck, K. Jeonghun, K.T. Yun, A.H.M. Shahriar, K. Sang-Woo, K.J. Ho, *All-in-one energy harvesting and storage devices*, *J. Mater. Chem. A* (2016) 7983–7999.

Presently, four primary effects, namely, piezoelectric, triboelectric, pyroelectric, and thermoelectric, are employed to develop nanogenerators having potential application in different sectors (Fig. 8.3 [6] and Fig. 8.4 [7]).

8.3 Piezoelectric nanogenerator

In some materials, if stress is applied, their atomic structure is altered prompting the formation of dipole moment, which leads to the generation of a voltage difference across the material. This type of material is called piezoelectric material, and the said effect is known as the direct piezoelectric

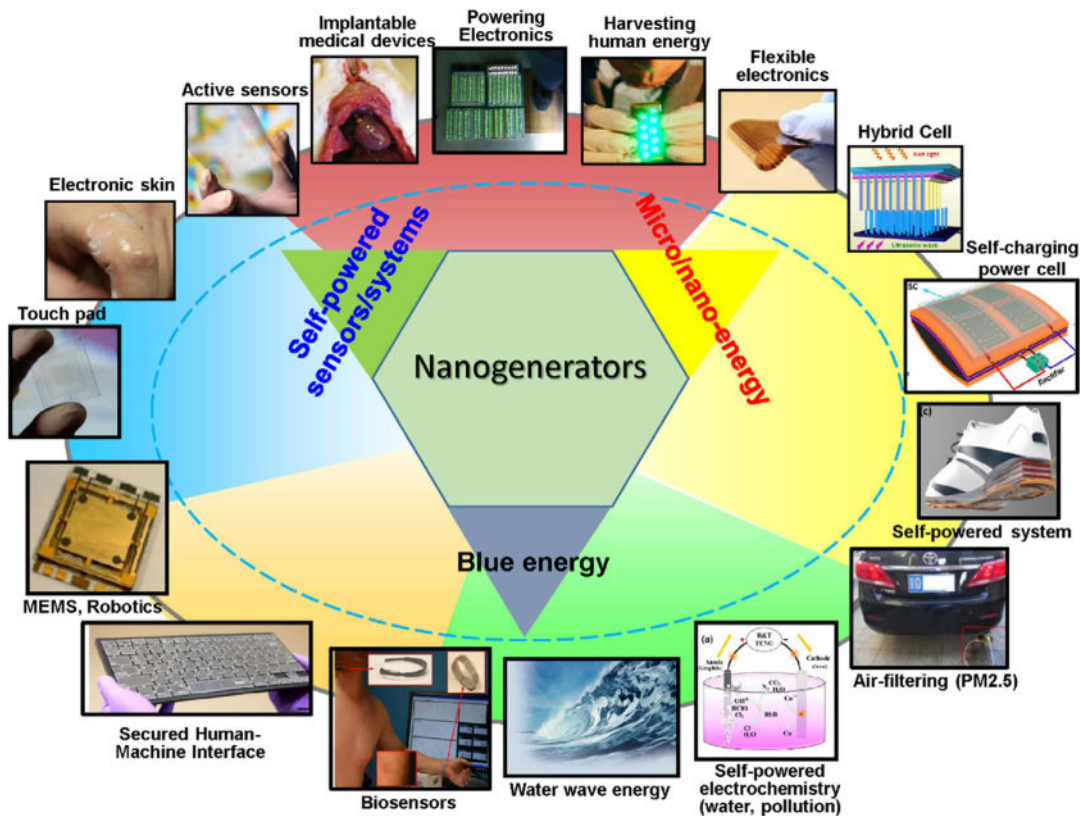


FIGURE 8.4

Different application sectors of piezoelectric, triboelectric, pyroelectric, and thermoelectric nanogenerators.

From W.Z. Lin, Nanogenerators, self-powered systems, blue energy, piezotronics and piezo-phototronics—a recall on the original thoughts for coining these fields, Nano Energy (2018) 477–483.

effect. However, if electrical polarization occurs within piezoelectric material, then material deformation takes place. This is known as a converse piezoelectric effect (Fig. 8.5) [8]

A piezoelectric nanogenerator (PENG) is an energy harvesting nanodevice, which can convert external mechanical energy into electrical energy employing the piezoelectric effect within a nanostructure piezoelectric material. PENG was first developed in 2006 by Wang's group [9]. The basic working principle of a PENG relies on the piezopotential, which is produced within the piezoelectric material. In general, two electrodes are connected at the opposite sides of the piezoelectric material. Initially, the Fermi levels of the two electrodes are balanced electrostatically. When strain is employed to the material by external means, the piezopotential is developed within the material producing a difference in-between the internal and external Fermi levels at the contacts. To nullify the differences in-between the Fermi levels, the electrons start to flow through external circuits in-between two electrodes till two electrodes are electrostatically rebalanced. External mechanical

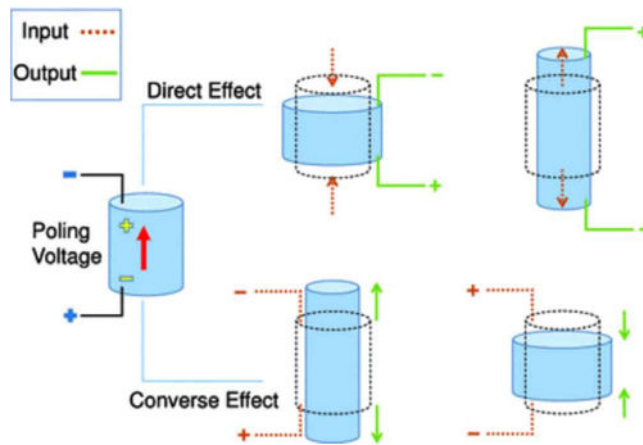


FIGURE 8.5

Direct and converse effects in piezoelectric ceramic [8].

From A. Jbaily, R.W. Yeung, *Piezoelectric devices for ocean energy: a brief survey*, *J. Ocean Eng. Mar. Energy* 1(1) (2015) 101–118.

forces can trigger strain within PENG in such a way that the strain undergoes periodical variations. This will give rise to an alternating current (AC) at the PENG output and establishes the PENG as a promising power source for the nanosystems. The external mechanical force can be applied in two directions: one is perpendicular to the nanowire and the other is parallel to the nanowire (Fig. 8.6) [10]. However, in both the cases, the top contact behaves as Schottky contact and the bottom contact behaves like an ohmic contact.

To boost the output power of the PENG, several nanowires should be integrated in such a way that deformation of each nanowire is perfectly synchronized. Till now, there are two types of structures of PENG, namely, lateral-nanowire integrated NG (LING) [11] and vertical-nanowire integrated NG (VING) [12] (Fig. 8.7) [10].

In LING, the nanowires are grown parallel to a flexible substrate and during bending deformation all the nanowires are deformed synchronously with the substrate, resulting in an elevated output power. While in VING, the device is fabricated directly on vertically grown nanowire arrays and it can produce energy from synchronous compression deformation of the NG.

Different piezoelectric materials such as lead zirconatetitanate [13], barium titanate [14], zinc oxide [15], polyvinylidene fluoride [16], cadmium sulfide [17], and molybdenum disulfide [18] have been used for the fabrication of PENG.

8.4 Triboelectric nanogenerator

Some materials get electrically charged when they make frictional contact with another dissimilar material [19]. This kind of contact-induced electrification is known as the triboelectric effect

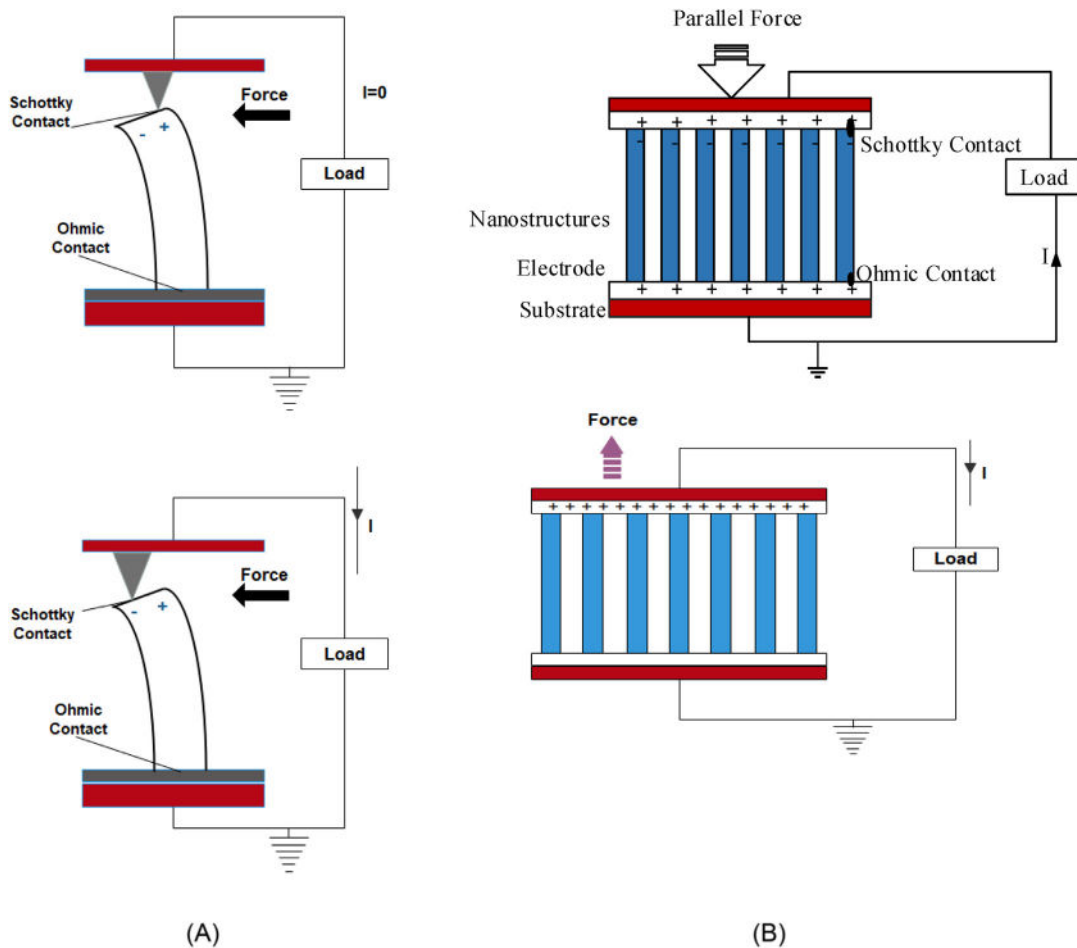


FIGURE 8.6

Different mechanism of operation of PENG: (left) Force exerted perpendicular to the growth of the nanowire and (right) force exerted parallel to the growth of the nanowire. *PENG*, piezoelectric nanogenerator.

From S.I. Sridhar, A.V. Chockalingam, O.K.S. Prakash, M. Faizal, R. Saidur, *Nanogenerators as a sustainable power source: state of art, applications, and challenges, Nanomaterials*, 9 (2019) 773.

(Fig. 8.8) [20]. After physical contact, the materials become oppositely charged, while the strength of the charges is different for different materials [21]

Based on triboelectrification and electrostatic induction effects, Wang's group [22] first put forward the idea of triboelectric nanogenerator (TENG) in 2012. There are four basic modes for TENG, namely, vertical contact-separation (CS) mode [23], lateral-sliding (LS) mode [24], single-electrode (SE) mode [25], and freestanding triboelectric-layer (FT) mode [26]. In all the four kinds of TENGs, there is a minimum of one pair of triboelectric surfaces with at least two electrodes (for

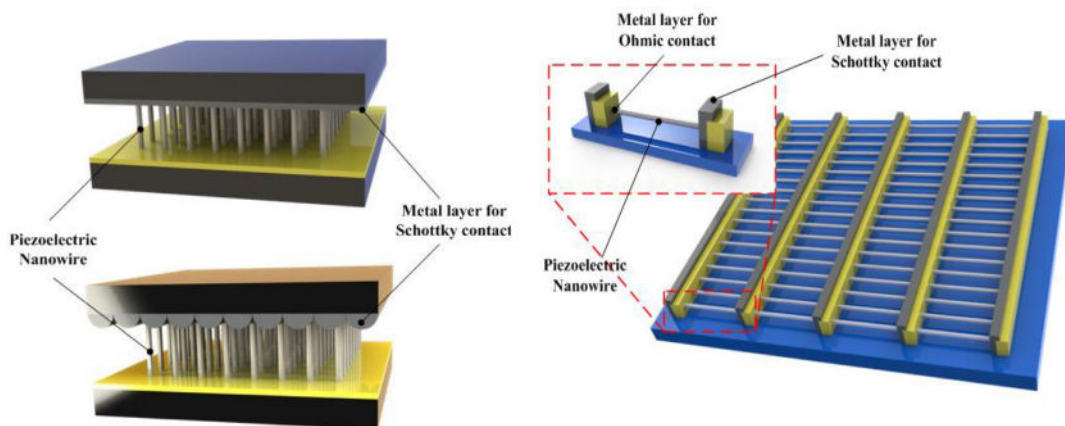


FIGURE 8.7

Different structures of PENG: (left) VING and (right) LING. *LING*, lateral-nanowire integrated nanogenerator; *PENG*, piezoelectric nanogenerator; *VING*, vertical-nanowire integrated nanogenerator.

From S.I. Sridhar, A.V. Chockalingam, O.K.S. Prakash, M. Faizal, R. Saidur, *Nanogenerators as a sustainable power source: state of art, applications, and challenges, Nanomaterials*, 9 (2019) 773.

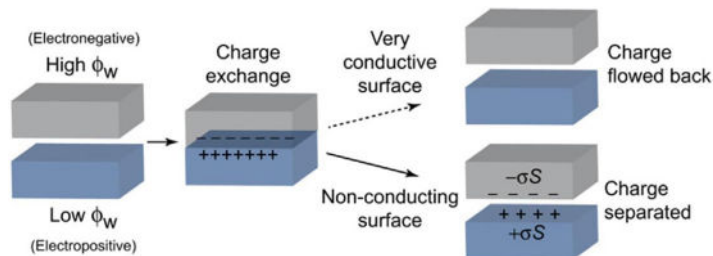


FIGURE 8.8

Triboelectric charge generation.

From P. Jun, K.S. Dongmin, S.G. Jeffrey, *Optimization principles and the figure of merit for triboelectric generators, Sci. Adv.* (2017) eaap8576.

SE mode, the ground is the other electrode). In the triboelectric effect, transport of electrostatic charges occurs from one surface to the other. Upon displacement of one of the triboelectric surfaces, the electrostatic status of the system changes resulting in the generation of the potential difference in-between the two electrodes. Subsequently, the generated potential difference causes a current to flow via the external circuit to balance the electrostatic status. Displacement of the triboelectric layers in the opposite direction creates a reverse potential difference in-between the electrodes, and therefore the current flows in the opposite direction. Thus an AC output is generated from the TENG via a periodical displacement of triboelectric layers. The triggering process is different

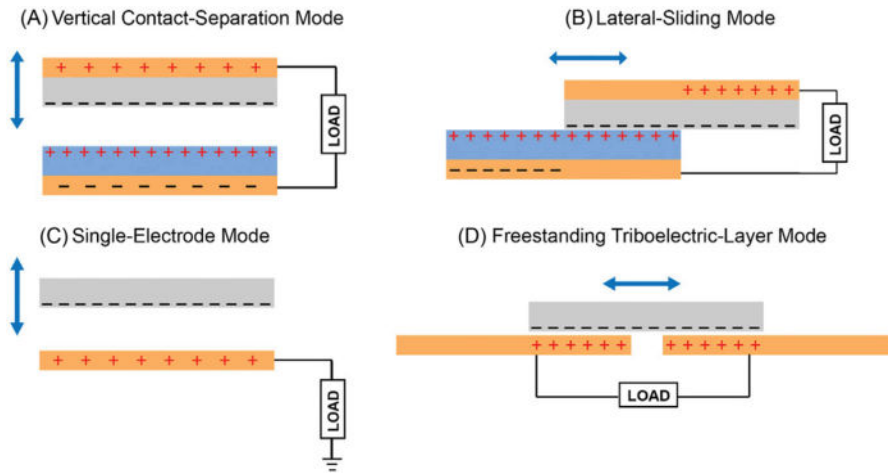


FIGURE 8.9

Four working modes of TENG. (A) Vertical CS mode, (B) LS mode, (C) SE mode, and (D) FT mode. CS, contact-separation; FT, freestanding triboelectric-layer; LS, lateral-sliding; SE, single-electrode; TENG, triboelectric nanogenerator.

From C. Wu, A.C. Wang, W. Ding, H. Guo, Z.L. Wang, *Triboelectric nanogenerator: a foundation of the energy for the new era*, *Adv. Energy Mater.* (2019) 1802906.

in all the four modes of TENG (Fig. 8.9) [27]. Contact and separation process of the two triboelectric layers triggers CS mode while relative sliding between triboelectric layers is responsible for the triggering of LS mode. In both CS and LS mode TENG, the external load is connected between the back electrodes of moving triboelectric layers and thereby imposing a limitation in the movement of the triboelectric layers. However, this limitation is waived off in the SE and FT mode of operation. In SE mode, a triboelectric layer moves freely with respect to one static electrode, while in FT mode a triboelectric layer moves freely between the two static electrodes to trigger the NG. To increase the output power of TENG via structural optimization, different structures like the multi-layer integrations [28] and grating structures [29] have been fabricated.

Different natural and ecofriendly materials that can be used to fabricate TENG are described in recent reviews by Slabov et al. [30] and Kim et al. [31].

8.5 Pyroelectric nanogenerator

The time-dependent temperature fluctuation often causes spontaneous polarization in certain anisotropic solids, which is known as the pyroelectric effect. The key parameter of the pyroelectric effect is the pyroelectric coefficient, which can be described as the differential change in spontaneous polarization owing to an alteration in temperature. The pyroelectric coefficient is the attribute of two phenomena, namely, primary pyroelectric effect and secondary pyroelectric effect [32]. If all the dimensions of a material remain constant (strain-free case), then the primary pyroelectric

coefficient is employed to express the amount of charges generated due to an alteration in temperature. On the other hand, if the dimensions of a material are altered due to the variation in temperature, then such anisotropic deformation of the material will produce a strain causing an additional contribution of piezoelectrically induced charges. This process is called secondary pyroelectric effect. In lead zirconate titanate, potassium niobate, barium titanate, and some other ferroelectric materials, the primary pyroelectric effect dominates, while in zinc oxide, cadmium sulfide, and some other wurtzite-type materials the secondary pyroelectric effect will predominate. Based on the pyroelectric effect, Wang's group [33] devised the first pyroelectric nanogenerator (PyENG) in 2012. The principle of generation of current via primary pyroelectric coefficient can be explained through the example of potassium niobate nanowire PyENG [34]. In potassium niobate, dipole moments readily exist along with the spontaneous polarization density (Fig. 8.10, top). With increasing temperature, the random oscillations of the ions

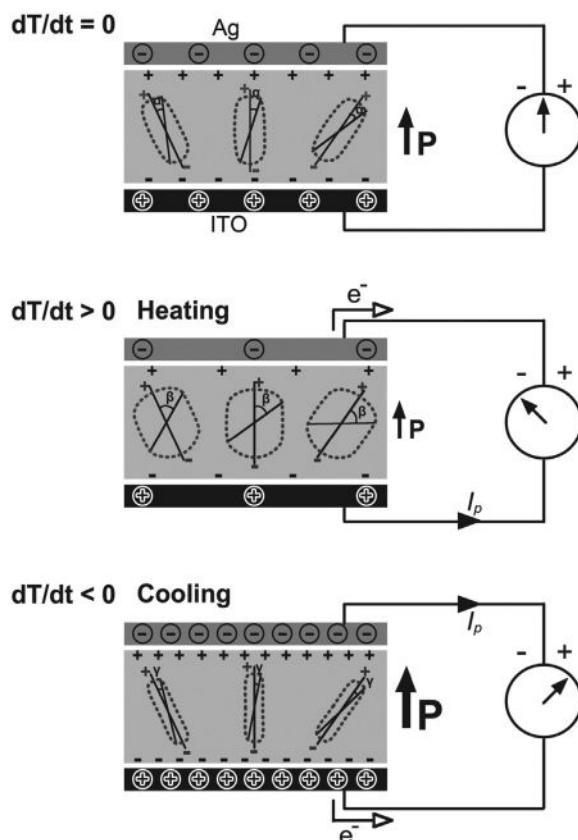


FIGURE 8.10

Primary pyroelectric effect.

From Y. Yang, J.H. Jung, B.K. Yun, F. Zhang, K.C. Pradel, W. Guo, et al., *Flexible pyroelectric nanogenerators using a composite structure of lead-free KNbO₃ nanowires*, *Adv. Mater.* 24(39) (2012) 5357–5362.

will intensify with a greater magnitude of spread around their corresponding aligning axes. This causes a reduction in effective dipole moments, and consequently the polarization density is decreased [35]. To regain the previous electrostatic status, charge carriers flow through the external circuit (Fig. 8.10, middle). Even if the PyENG is cooled down from ambient temperature, the oscillations of the ions are reduced with a smaller amplitude of spread across their respective aligning axes and thereby causing an enhancement in effective dipole moments. The resulting increase in polarization density prompts the flow of charge in the reverse direction (Fig. 8.10, bottom).

The principle of generation of current via secondary pyroelectric coefficient can be explained via the example of zinc oxide nanowire [33]. PyENG is vertically grown zinc oxide nanowires sandwiched between two electrodes. With the increase in temperature, a pyroelectric potential is created along zinc oxide nanowire, thus one electrode becomes electrically positive and the other electrode becomes electrically negative. As the Fermi level of the electrically negative electrode is enhanced, it will drive the electrons to flow from the negative electrode to the electrically positive electrode. After the temperature goes down to the initial value, the electrons accumulated at the positive electrode are released and flow back to the negative electrode as the pyroelectric electrical potential is faded away. Here, a difference in piezoelectric potential is created across the material by the anisotropic thermal deformation and because of the emerged potential difference, the electrons flow through the external circuit. Thus the output of the secondary pyroelectric effect-based nanogenerator is actually the combined effect of the piezoelectric coefficient and the anisotropic thermal deformation of the material (Fig. 8.11) [35].

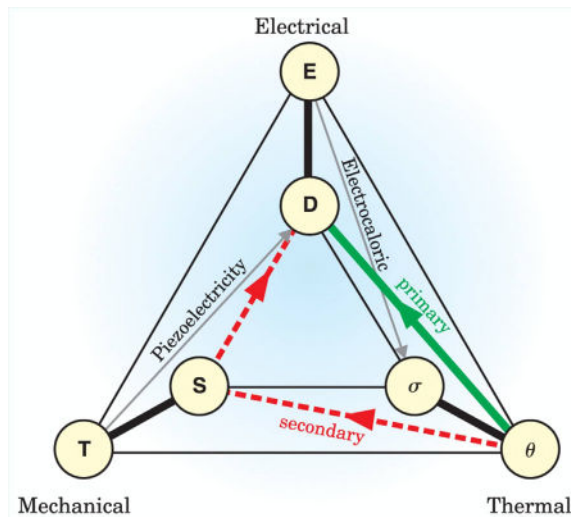


FIGURE 8.11

Secondary pyroelectric effect (where D denotes electrical displacement, S denotes constant strain, E denotes electric field, T denotes elastic stress, σ denotes entropy, and θ denotes temperature).

From S.B. Lang, Pyroelectricity: from ancient curiosity to modern imaging tool, Phys. Today 58(8) (2005) 31–36.

Different materials like triglycine sulfate [36], gallium nitride [37], zinc oxide [33], and perovskite-based pyroelectrics have been used to fabricate PyENG.

8.6 Thermoelectric nanogenerator

If two interconnected dissimilar conductors are maintained at different temperatures, then a potential difference is created between the conductors that is directly proportional to the temperature difference and such potential difference results in the flow of current in the loop. This thermoelectric phenomenon is called the Seebeck effect (Fig. 8.12) [38].

The Seebeck effect is utilized to fabricate thermoelectric nanogenerator (ThENG). If a thermal gradient exists in the environment, then a ThENG can convert the heat into electrical energy. In 2012, Wang's group first fabricated ThENG using single Sb-doped ZnO micro/nanobelts [39] (Fig. 8.13). They had placed the ZnO belt on a glass substrate and used silver paste to fix the two ends, which eventually acted as electrodes with a separation of 3 mm. They found that 30 K temperature difference between two electrodes of ThENG can produce an output current and voltage of about 194 nA and 10 mV, respectively.

To explain this phenomenon, a π -type model can be employed. In the π -type model, the structure is made up of one p-type and one n-type semiconductor, which are connected via a conducting wire/strip to complete the electrical circuit (Fig. 8.14) [40]. When one side of p-type and n-type material is heated and another one is cooled, the majority charge carriers (holes) of p-type materials

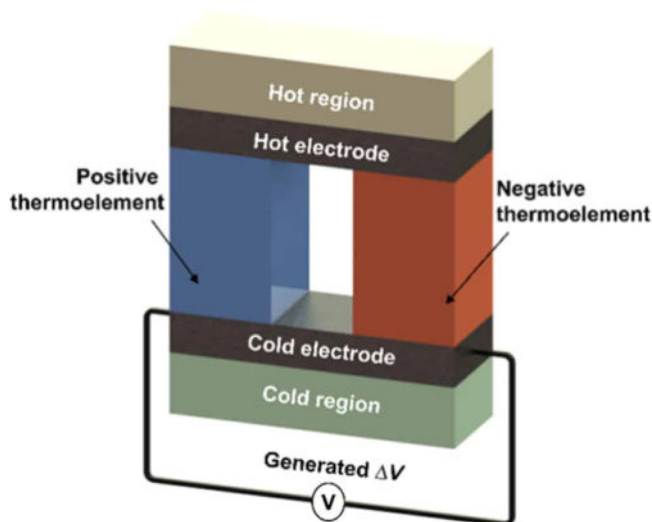


FIGURE 8.12

Diagram of an energy generation mechanism using the thermoelectric effect.

From K.V. Selvan, M.N. Hasan, M.S. Mohamed Ali, Methodological reviews and analyses on the emerging research trends and progresses of thermoelectric generators, Int. J. Energy Res. 43(1) (2019) 113–140.

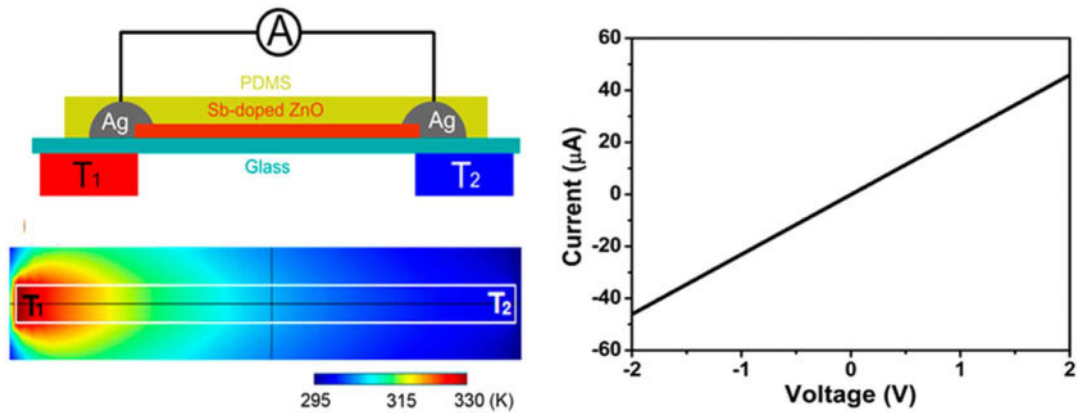


FIGURE 8.13

A ZnO ThENG based on the Seebeck effect. (Top left) Schematic diagram of a single Sb-doped ZnO microbelt NG. (Bottom left) Calculated temperature distribution along a glass substrate. (Right) I – V characteristic of a fabricated NG. NG, nanogenerator; ThENG, thermoelectric nanogenerator.

From Y. Yang, K.C. Pradel, Q. Jing, J.M. Wu, F. Zhang, Y. Zhou, et al., *Thermoelectric nanogenerators based on single Sb-doped ZnO micro/nanobelts*, ACS Nano 6(8) (2012) 6984–6989.

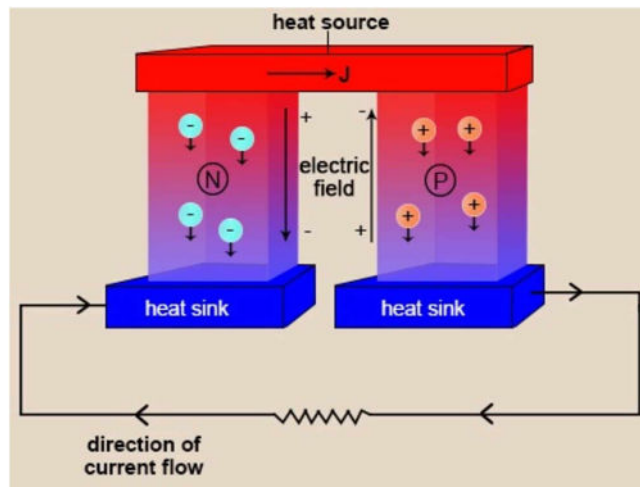


FIGURE 8.14

A π -type model to explain the working principle of ThENG. ThENG, thermoelectric nanogenerator.

From A simple explanation of Seebeck effect with its applications. <<https://sciencestruck.com/seebeck-effect-with-applications/>>, 2014 (accessed 20.05.2020).

and that (electrons) of n-type materials will diffuse from the hot side to the cold side. This diffusion process results in building-up charge carriers at the cold end. Such build-up of charge carriers at one end produces a potential difference across the semiconductor, proportional to the temperature difference across the semiconductor. If the cold ends of both the semiconductors are electrically connected, then a current flows from the p-type material to the n-type material.

8.7 Blue energy harvesting using nanogenerators

As the futuristic growth of science and technology is confronting the dual challenge of energy crisis and carbon pollution, renewable energy sources must be extensively explored and the use of fossil fuels should be restricted to a minimum. Among the different renewable energy resources, ocean energy is one of the least explored renewable energy sources on the earth. The total blue energy content of ocean was estimated to be 7.66×10^{13} W [41]. Both the thermal and mechanical energy can be harvested from the ocean. The temperature gradient that exists across the warm surface waters and the cool deeper waters can be utilized to generate thermal energy and mechanical energy can be harvested from the tides, waves, and currents of the ocean. The blue energy has several advantages over the other available renewable energy resources. First, blue energy is invariant to weather, time of the day, or temperature [42]. Second, tides, waves, and currents are predictable globally and more reliable than wind and solar energy. Finally, harvesting blue energy requires the minimal use of land and small environmental interaction, thereby offering one of the most lenient techniques for large-scale, ecofriendly, and sustainable electricity generation [43]. Among different NGs, TENG has a huge potential for harvesting blue energy [44]. TENG can effectively harvest blue energy even at frequencies <5 Hz, which is perfectly suitable to harvest energy from a low-frequency ocean wave [45]. Since the invention of TENG, much effort has been made to harvest blue energy via various designs of prototypes.

8.7.1 Water-involved TENG

In this type of TENG, water is used as one of the triboelectric materials and liquid–solid contact electrification harvests the output energy (Fig. 8.15) [46]. The first water-involved TENG was reported by Lin et al. [47] in 2013, where periodic contact and separation between water and polydimethylsiloxane (PDMS) pyramid array give rise to the output energy. The frequency response test revealed that optimized power density is 50 mW/m^2 at 5 Hz, while the peak power density is nearly 0.13 W/m^2 . Here, the water remaining on the PDMS array will affect the output power. To overcome this hurdle, Zong-Hong et al. [48] modified their design and used superhydrophobic polytetrafluoroethylene (PTFE) in place of PDMS and could achieve an output power of 20 mW/cm^2 . Later, different kinds of polymer material with varied structures were employed by Guang et al. [49] and Zhao et al. [50] for the fabrication of water involved TENG. By modification of the structures, they were able to achieve the output power up to 1.1 mW, while initially it was only 0.12 mW. When water flows through the air or an insulating tube, because of the contact with the air/solid surface, triboelectric charges will be induced on its surface and the water will contain the mechanical energy as well as the electrostatic energy. For harvesting the mechanical and

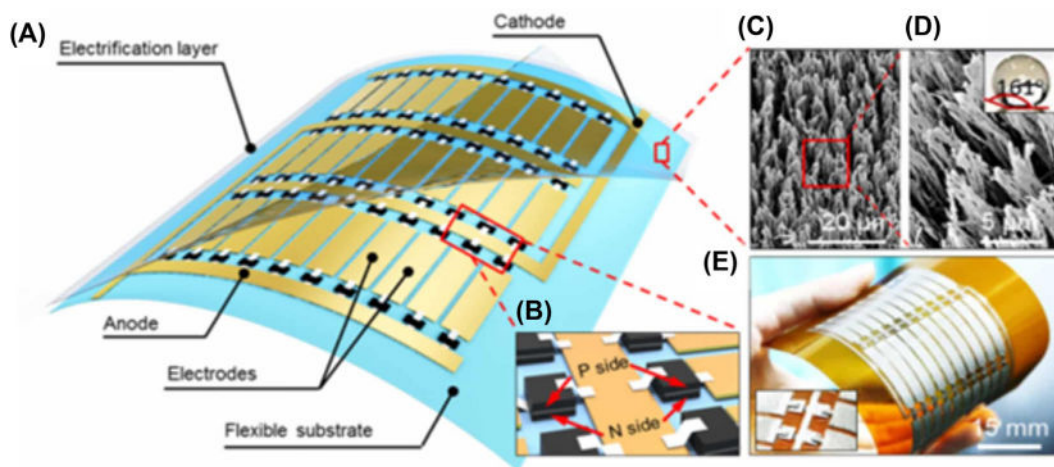


FIGURE 8.15

Structure of a networked integrated triboelectric nanogenerator (NI-TENG). (A) Schematic diagram of an NI-TENG. (B) Enlarged sketch of the arrayed bridge rectifiers. (C) SEM image of the PTFE nanowires on the electrification layer. (D) Enlarged view of the nanowires, inset: contact angle on the nanostructured surface. (E) Picture of a bendable as-fabricated NI-TENG, inset: Enlarged view of the rectifying diodes. *PTFE*, polytetrafluoroethylene; *SEM*, scanning electron microscope.

From X.J. Zhao, S.Y. Kuang, Z.L. Wang, G. Zhu, *Highly adaptive solid-liquid interfacing triboelectric nanogenerator for harvesting diverse water wave energy*, *ACS Nano* 12(5) (2018) 4280–4285.

electrostatic energies of flowing water, simultaneously, a dual-mode TENG was fabricated by Zong-Hong et al. [51], employing superhydrophobic TiO_2 layer with hierarchical micro/nanostructures. Gang et al. [52] developed a dual-mode TENG consisting of a disk-TENG part and a water-TENG part. The water-TENG was composed of eight wheel blades covered by a PTFE film to harvest the electrostatic energy from flowing water. Kinetic energy can be harvested through the rotational movement of disk-TENG caused by the flowing water. A hybrid TENG comprising interfacial electrification enabled TENG and an impact-TENG was developed by Yuanjie et al. [53] with an internal wavy-electrode structure to harvest mechanical energy and electrostatic energy from water. A novel cylinder-shaped structure TENG, based on contact electrification in-between water and PTFE filtration membranes, was proposed by Xiaolong et al. [54]. The recommended device can achieve a short-circuit current of $1.5 \mu\text{A}$ and an open-circuit voltage of 12 V. Fluorinated ethylene propylene (FEP) nanowire-based TENG was proposed by Xiaoyi et al. [55]. Due to the presence of nanowires the contact area had been significantly increased causing more friction between polymer and water which in turn produced an output current of $10 \mu\text{A}$ and an output voltage of 200 V. Shi et al. Qiongfeng et al. [56] proposed a buoy ball type symmetric spherical-shaped water-based TENG employing Al electrodes wrapped by PTFE thin films to produce the arbitrary directional and irregular water wave energy. A U tube-shaped TENG based on FEP was fabricated by Pan et al. [57] to harvest blue energy. A further modified structure with sandwich-like water-FEP U-tube TENG was developed to harvest blue energy with a power density

of 2.04 W/m^3 . Minyi et al. [58] developed a tower-shaped TENG, which was composed of multiple units, made of PETF balls and nylon film-coated arc surface, connected in parallel. The tower-shaped TENG containing 10 units in parallel can harvest blue energy from random directions with a power density of 10.6 W/m^3 . Blue energy harvesting by regular fabric using a nontoxic and low-cost hydrophobic coating of hydrophobic cellulose oleoyl ester nanoparticles was demonstrated by Jiaqing et al. [59]. Xiaoyi et al. [60] designed and fabricated a buoy-like liquid–solid contact-based TENG, which magnifies the output energy via increased friction by 48.7 times, in comparison to the solid–solid contact-based TENG having an identical area. Jinhui et al. [61] developed a novel liquid–liquid TENG, which can harvest blue energy with a peak power of 137.4 nW by passing a liquid droplet through a freely suspended liquid membrane.

However, one major problem of water involved TENG is that the seawater can corrode polymer films via direct contact. Thus to overcome this problem researchers are intending to use fully enclosed TENG to harvest blue energy as discussed in the next subsection.

8.7.2 Nonwater-involved TENG

In general, a waterproof layer is employed in the nonwater-involved TENG (Fig. 8.16) [62]. In July 2013, the first nonwater-involved TENG was fabricated in a fully enclosed spherical shell by Ya et al. [63] using PTFE-polyamide films. A suspended three-dimensional spiral structured TENG was designed and fabricated by Youfan et al. [64] for harvesting blue energy with a power density

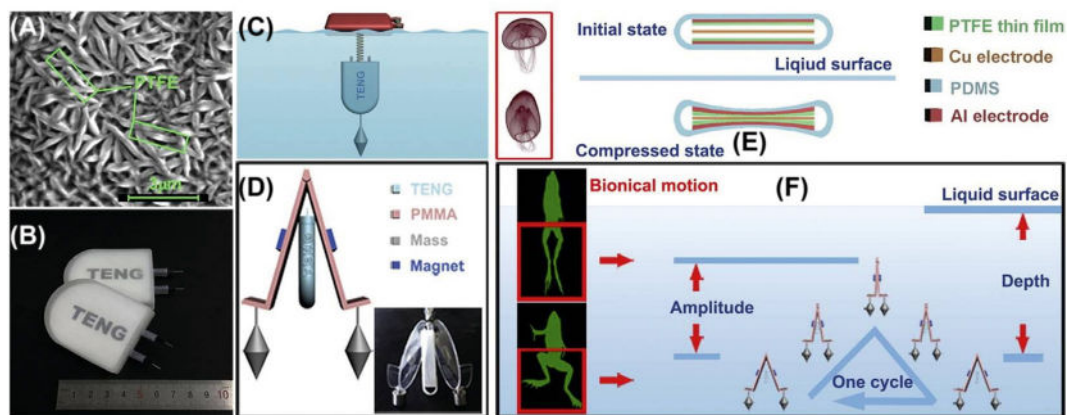


FIGURE 8.16

The structure and fabrication process of the bionic-jellyfish triboelectric nanogenerator (bjTENG). (A) SEM images of the tribo-material PTFE thin film, (B) digital image of bjTENG, and (C) illustration of an application. (D) Schematic diagrams of the optimized structure. (E) Working process of the interface self-powered fluctuation sensor and (F) five-step working process of the undersea bjTENG. PTFE, polytetrafluoroethylene; SEM, scanning electron microscope.

From B.D. Chen, W. Tang, C. He, C.R. Deng, L.J. Yang, L.P. Zhu, et al., *Water wave energy harvesting and self-powered liquid-surface fluctuation sensing based on bionic-jellyfish triboelectric nanogenerator*, *Mater. Today* 21(1) (2018) 88–97.

of 2.76 W/m^2 . Xiaonan et al. [65] developed a wavy-structured TENG comprising a Cu-Kapton-Cu film sandwiched in-between two flat nanostructured PTFE to collect blue energy with a power density of 0.4 W/m^2 . Zhang et al. [66] further modified the structure and designed a regular dodecahedron device containing 12 sets of wavy-structured TENGs. Each TENG consists of a wavy-structured Cu-Kapton-Cu film sandwiched between two flat nanostructured FEP thin films. This TENG can harvest 0.64 MW power from 1 km^2 surface area of water. Lin et al. [67] created a network of TENGs, which can generate an average output power of 1.15 MW from 1 km^2 surface area. A water treatment system was designed by Qianwen et al. [68] employing a TENG, which will harvest energy from the water itself. Liang et al. [69] designed an array of integrated TENG based on air-driven membrane structures with an optimized peak power density of 13.23 W/m^3 . Here air pressure was used to distribute and transfer harvested water wave energy and a spring-levitated oscillator helped it to achieve resonance in a short time-span. Jiang et al. Tao et al. [70] developed a spring-assisted TENG comprising two Cu-PTFE-based TENGs connected through spring. They found that due to the presence of the spring, the energy conversion efficiency can be augmented by 150.3%. The spring-based structure was modified by Xiao et al. [71] by employing silicone rubber/carbon black composite electrode, which can provide better contact with the dielectric film. While triggered by the water waves, it can generate output with a maximum power density of 2.40 W/m^3 . Later they fabricated TENG array consisting of four spherical TENGs [72] based on the spring-assisted multilayered structure to harvest power up to 15.97 mW . A box-shaped TENG consisting of wavy-structured Cu-Kapton-Cu and FEP films, with an enclosed metal ball, was designed and fabricated by Jiang et al. [73]. Later they optimized the charging behavior under the enclosed ball collision and direct water wave impact [74]. They reported that in case of the direct water wave impact, deformation depth governs the energy storage efficiency, whereas for the enclosed ball collision the size of the ball is responsible for energy storage efficiency. A ball-shell structured TENG network was developed by Xu et al. [75] with flexible connections. They found that the charge output of the coupled units is 10 times more in comparison to that without coupling. Lin et al. [76] devised a new methodology of soft-surface-contact based spherical TENG employing silicone rubber to maximize the transferred charge during the triboelectric effect by 10-fold in comparison to conventional PTFE-based hard-contact TENG. A torus structured TENG enclosing a ball was fabricated by Wenbo et al. [77], which can harvest blue energy with a power density of 0.21 W/m^2 . A self-assembly of self-healable and reconfigurable TENG network was developed by Yang et al. [78] with an average power density of 8.69 W/m^3 . A pendulum structured robust TENG was fabricated by Zhiming et al. [79], which can deliver frequency multiplied output. Zhong et al. [80] fabricated a TENG with an open book-like structure. Owing to its unique structure, many TENGs can be accommodated in a small area with high packing density to harvest blue energy with a peak power density of 7.45 W/m^3 . To harvest multidirectional blue energy, Rui et al. [81] designed a butterfly-shaped TENG using spring-assisted four-bar linkage to achieve a maximum output power density of 9.559 W/m^3 . A bimodal, highly stretchable, superhydrophobic TENG was developed by Xiaoliang et al. [82], which was made of an ionic conductor and hierarchical micro-nanostructures with self-cleaning properties. The proposed TENG can harvest blue energy with a power density of 0.36 mW . The principle of the pendulum was applied to fabricate a TENG with a compact disk-track structure to achieve a peak power density of 14.71 W/m^3 via area contact mechanism. An oblate spheroidal TENG was designed and fabricated by Liu et al. Guanlin et al. [83], which is much superior compared to the traditional sphere shell and can harvest blue energy with a

power density of 21.356 mW. The performance of spherical-shaped TENG was further improved by Liang et al. [84] using a spring-assisted multilayered structure with integrated power management module (PMM) to control the harvested energy.

8.8 Summary and perspective

Mankind moves toward modernization of each and every aspect of technology and modernization needs energy. However, the conventional energies are limited and thus the continuous proliferation of technological progress necessitates alternative one. The process to harvest alternative energy should be inexpensive, self-powered, ecofriendly, sustainable, and preferably maintenance-free for a seamless growth of technology. The evolution of the nanogenerator in 2006 created a revolution in harvesting alternative energy from the ambient environment by various means. The four physical processes, namely, piezoelectric effect, triboelectric effect, pyroelectric effect, and thermoelectric effects, were employed in the nanogenerators to harvest energy. The rapid growth in the development of the different nanogenerators has marked the foundation for self-powered modern electronic systems. However, to harvest ambient energy like blue energy on a large scale, nanogenerator with long durability, efficient energy conversion, and enhanced output power density is desirable. The futuristic research on nanogenerators should be focused on the efficient integration methodology and improved power management module (PMM).

References

- [1] BP Energy Outlook. Energy economics. <<https://www.bp.com/en/global/corporate/energy-economics/energy-outlook.html>>, 2019 (accessed 31.03.20).
- [2] BP global. <<https://www.bp.com/en/global/corporate.html>>, 2019 (accessed 27.05.20).
- [3] F. Gazeau, C. Baravian, J.C. Bacri, R. Perzynski, M.I. Shliomis, Energy conversion in ferrofluids: magnetic nanoparticles as motors or generators, *Phys. Rev. E Stat. Phys. Plasmas Fluids Relat. Interdiscip. Top.* 56 (1) (1997) 614–618. Available from: <https://doi.org/10.1103/PhysRevE.56.614>.
- [4] W.Z. Lin, On the first principle theory of nanogenerators from Maxwell's equations, *Nano Energy* (2020) 104272. Available from: <https://doi.org/10.1016/j.nanoen.2019.104272>.
- [5] Z.L. Wang, On Maxwell's displacement current for energy and sensors: the origin of nanogenerators, *Mater. Today* 20 (2) (2017) 74–82. Available from: <https://doi.org/10.1016/j.mattod.2016.12.001>.
- [6] L. Ju-Hyuck, K. Jeonghun, K.T. Yun, A.H.M. Shahriar, K. Sang-Woo, K.J. Ho, All-in-one energy harvesting and storage devices, *J. Mater. Chem. A* (2016) 7983–7999. Available from: <https://doi.org/10.1039/C6TA01229A>.
- [7] W.Z. Lin, Nanogenerators, self-powered systems, blue energy, piezotronics and piezo-phototronics—a recall on the original thoughts for coining these fields, *Nano Energy* (2018) 477–483. Available from: <https://doi.org/10.1016/j.nanoen.2018.09.068>.
- [8] A. Jbaily, R.W. Yeung, Piezoelectric devices for ocean energy: a brief survey, *J. Ocean Eng. Mar. Energy* 1 (1) (2015) 101–118. Available from: <https://doi.org/10.1007/s40722-014-0008-9>.
- [9] Z.L. Wang, J. Song, Piezoelectric nanogenerators based on zinc oxide nanowire arrays, *Science* 312 (5771) (2006) 242–246. Available from: <https://doi.org/10.1126/science.1124005>.

- [10] S.I. Sridhar, A.V. Chockalingam, O.K.S. Prakash, M. Faizal, R. Saidur, Nanogenerators as a sustainable power source: state of art, applications, and challenges, *Nanomaterials* 9 (2019) 773. Available from: <https://doi.org/10.3390/nano9050773>.
- [11] G. Zhu, R. Yang, S. Wang, Z.L. Wang, Flexible high-output nanogenerator based on lateral ZnO nanowire array, *Nano Lett.* 10 (8) (2010) 3151–3155. Available from: <https://doi.org/10.1021/nl101973h>.
- [12] H. Youfan, Z. Yan, X. Chen, L. Long, S.R. L. W.Z. Lin, Self-powered system with wireless data transmission, *Nano Lett.* (2011) 2572–2577. Available from: <https://doi.org/10.1021/nl201505c>.
- [13] L. Horim, K. Hoyeon, K.D. Young, S. Yongsok, Pure piezoelectricity generation by a flexible nanogenerator based on lead zirconatetitanate nanofibers, *ACS Omega* (2019) 2610–2617. Available from: <https://doi.org/10.1021/acsomega.8b03325>.
- [14] S. Saqib, K. Do-II, D.L. Thai, N.M. Triet, M. Shoaib, Y. Won-Sub, et al., High-performance flexible lead-free nanocomposite piezoelectric nanogenerator for biomechanical energy harvesting and storage, *Nano Energy* (2015) 177–185. Available from: <https://doi.org/10.1016/j.nanoen.2015.04.030>.
- [15] K. Jasleen, S. Harminder, Synthesis and fabrication of zinc oxide nanostrands based piezoelectric nanogenerator, *J. Mater. Sci. Mater. Electron.* (2019) 4437–4445. Available from: <https://doi.org/10.1007/s10854-019-00732-3>.
- [16] Y. Jing, L. Min, J.Y. Gyu, K. Weimin, L. Lan, Z. Yixia, et al., Performance enhancements in poly(vinylidene fluoride)-based piezoelectric nanogenerators for efficient energy harvesting, *Nano Energy* (2019) 662–692. Available from: <https://doi.org/10.1016/j.nanoen.2018.12.010>.
- [17] Y.F. Lin, J. Song, Y. Ding, S.Y. Lu, Z.L. Wang, Piezoelectric nanogenerator using CdS nanowires, *Appl. Phys. Lett.* 92 (2) (2008). Available from: <https://doi.org/10.1063/1.2831901>.
- [18] H. James, W.Z. Lin, L. Yilei, Z. Fan, L. Long, N. Simiao, et al., Piezoelectricity of single-atomic-layer MoS₂ for energy conversion and piezotronics, *Nature* (2014) 470–474. Available from: <https://doi.org/10.1038/nature13792>.
- [19] R.G. Horn, D.T. Smith, Contact electrification and adhesion between dissimilar materials, *Science* 256 (5055) (1992) 362–364. Available from: <https://doi.org/10.1126/science.256.5055.362>.
- [20] P. Jun, K.S. Dongmin, S.G. Jeffrey, Optimization principles and the figure of merit for triboelectric generators, *Sci. Adv.* (2017) eaap8576. Available from: <https://doi.org/10.1126/sciadv.aap8576>.
- [21] R.G. Horn, D.T. Smith, A. Grabbe, Contact electrification induced by monolayer modification of a surface and relation to acid-base interactions, *Nature* 366 (6454) (1993) 442–443. Available from: <https://doi.org/10.1038/366442a0>.
- [22] F. Feng-Ru, T. Zhong-Qun, L.W. Zhong, Flexible triboelectric generator, *Nano Energy* (2012) 328–334. Available from: <https://doi.org/10.1016/j.nanoen.2012.01.004>.
- [23] F.R. Fan, L. Lin, G. Zhu, W. Wu, R. Zhang, Z.L. Wang, Transparent triboelectric nanogenerators and self-powered pressure sensors based on micropatterned plastic films, *Nano Lett.* 12 (6) (2012) 3109–3114. Available from: <https://doi.org/10.1021/nl300988z>.
- [24] G. Zhu, J. Chen, Y. Liu, P. Bai, Y.S. Zhou, Q. Jing, et al., Linear-grating triboelectric generator based on sliding electrification, *Nano Lett.* 13 (5) (2013) 2282–2289. Available from: <https://doi.org/10.1021/nl4008985>.
- [25] Y. Yang, H. Zhang, J. Chen, Q. Jing, Y.S. Zhou, X. Wen, et al., Single-electrode-based sliding triboelectric nanogenerator for self-powered displacement vector sensor system, *ACS Nano* 7 (8) (2013) 7342–7351. Available from: <https://doi.org/10.1021/nn403021m>.
- [26] S. Wang, Y. Xie, S. Niu, L. Lin, Z.L. Wang, Freestanding triboelectric-layer-based nanogenerators for harvesting energy from a moving object or human motion in contact and non-contact modes, *Adv. Mater.* 26 (18) (2014) 2818–2824. Available from: <https://doi.org/10.1002/adma.201305303>.
- [27] C. Wu, A.C. Wang, W. Ding, H. Guo, Z.L. Wang, Triboelectric nanogenerator: a foundation of the energy for the new era, *Adv. Energy Mater.* (2019) 1802906. Available from: <https://doi.org/10.1002/aenm.201802906>.

- [28] P. Bai, G. Zhu, Z.H. Lin, Q. Jing, J. Chen, G. Zhang, et al., Integrated multilayered triboelectric nanogenerator for harvesting biomechanical energy from human motions, *ACS Nano* 7 (4) (2013) 3713–3719. Available from: <https://doi.org/10.1021/nn4007708>.
- [29] X. Yannan, W. Sihong, N. Simiao, L. Long, J. Qingshen, Y. Jin, et al., Grating-structured freestanding triboelectric-layer nanogenerator for harvesting mechanical energy at 85% total conversion efficiency, *Adv. Mater.* (2014) 6599–6607. Available from: <https://doi.org/10.1002/adma.201402428>.
- [30] V. Slabov, S. Kopyl, S. P. M.P.S. dos Santos, A.L. Kholkin, Natural and eco-friendly materials for triboelectric energy harvesting, *Nano Micro Lett.* (2020). Available from: <https://doi.org/10.1007/s40820-020-0373-y>.
- [31] D.W. Kim, J.H. Lee, J.K. Kim, U. Jeong, Material aspects of triboelectric energy generation and sensors, *NPG Asia Mater.* 12 (1) (2020). Available from: <https://doi.org/10.1038/s41427-019-0176-0>.
- [32] A.S. Bhalla, R.E. Newnham, Primary and secondary pyroelectricity, *Phys. Status Solidi A* 58 (1) (1980) K19–K24. Available from: <https://doi.org/10.1002/pssa.2210580146>.
- [33] Y. Yang, W. Guo, K.C. Pradel, G. Zhu, Y. Zhou, Y. Zhang, et al., Pyroelectric nanogenerators for harvesting thermoelectric energy, *Nano Lett.* 12 (6) (2012) 2833–2838. Available from: <https://doi.org/10.1021/nl3003039>.
- [34] Y. Yang, J.H. Jung, B.K. Yun, F. Zhang, K.C. Pradel, W. Guo, et al., Flexible pyroelectric nanogenerators using a composite structure of lead-free KNbO_3 nanowires, *Adv. Mater.* 24 (39) (2012) 5357–5362. Available from: <https://doi.org/10.1002/adma.201201414>.
- [35] S.B. Lang, Pyroelectricity: from ancient curiosity to modern imaging tool, *Phys. Today* 58 (8) (2005) 31–36. Available from: <https://doi.org/10.1063/1.2062916>.
- [36] R. Ghane-Motlagh, P. Woias, A pyroelectric thin film of oriented triglycine sulfate nano-crystals for thermal energy harvesting, *Smart Mater. Struct.* 28 (10) (2019). Available from: <https://doi.org/10.1088/1361-665X/ab3910>.
- [37] C.R. Bowen, J. Taylor, E. Leboulbar, D. Zabek, A. Chauhan, R. Vaish, Pyroelectric materials and devices for energy harvesting applications, *Energy Environ. Sci.* 7 (12) (2014) 3836–3856. Available from: <https://doi.org/10.1039/c4ee01759e>.
- [38] K.V. Selvan, M.N. Hasan, M.S. Mohamed Ali, Methodological reviews and analyses on the emerging research trends and progresses of thermoelectric generators, *Int. J. Energy Res.* 43 (1) (2019) 113–140. Available from: <https://doi.org/10.1002/er.4206>.
- [39] Y. Yang, K.C. Pradel, Q. Jing, J.M. Wu, F. Zhang, Y. Zhou, et al., Thermoelectric nanogenerators based on single Sb-doped ZnO micro/nanobelts, *ACS Nano* 6 (8) (2012) 6984–6989. Available from: <https://doi.org/10.1021/nn302481p>.
- [40] Science Struck A simple explanation of Seebeck effect with its applications. <<https://sciencestruck.com/seebeck-effect-with-applications>>, 2014 (accessed 20.05.2020).
- [41] E. Omar, A.-R. Haitham, B. Frede, Renewable energy resources: current status, future prospects and their enabling technology, *Renew. Sustain. Energy Rev.* (2014) 748–764. Available from: <https://doi.org/10.1016/j.rser.2014.07.113>.
- [42] A. F. d O. Falcão, Wave energy utilization: a review of the technologies, *Renew. Sustain. Energy Rev.* 14 (3) (2010) 899–918. Available from: <https://doi.org/10.1016/j.rser.2009.11.003>.
- [43] G.S. Bhuyan, World-wide status for harnessing ocean renewable resources, in: IEEE PES General Meeting, PES 2010, Canada, 2010. <<https://doi.org/10.1109/PES.2010.5589292>>.
- [44] W.Z. Lin, Triboelectric nanogenerators as new energy technology and self-powered sensors – Principles, problems and perspectives, *Faraday Discuss.* (2014) 447–458. Available from: <https://doi.org/10.1039/C4FD00159A>.
- [45] Z. Yunlong, G. Hengyu, W. Zhen, Y. Min-Hsin, H. Chenguo, W.Z. Lin, Harvesting low-frequency (<5 Hz) irregular mechanical energy: a possible killer application of triboelectric nanogenerator, *ACS Nano* (2016) 4797–4805. Available from: <https://doi.org/10.1021/acs.nano.6b01569>.

- [46] X.J. Zhao, S.Y. Kuang, Z.L. Wang, G. Zhu, Highly adaptive solid-liquid interfacing triboelectric nanogenerator for harvesting diverse water wave energy, *ACS Nano* 12 (5) (2018) 4280–4285. Available from: <https://doi.org/10.1021/acsnano.7b08716>.
- [47] Z.H. Lin, G. Cheng, L. Lin, S. Lee, Z.L. Wang, Water-solid surface contact electrification and its use for harvesting liquid-wave energy, *Angew. Int. Ed.* 52 (48) (2013) 12545–12549. Available from: <https://doi.org/10.1002/anie.201307249>.
- [48] L. Zong-Hong, C. Gang, L. Sangmin, P.K. C, W.Z. Lin, Harvesting water drop energy by a sequential contact-electrification and electrostatic-induction process, *Adv. Mater.* (2014) 4690–4696. Available from: <https://doi.org/10.1002/adma.201400373>.
- [49] Z. Guang, S. Yuanjie, B. Peng, C. Jun, J. Qingshen, Y. Weiqing, et al., Harvesting water wave energy by asymmetric screening of electrostatic charges on a nanostructured hydrophobic thin-film surface, *ACS Nano* (2014) 6031–6037. Available from: <https://doi.org/10.1021/nn5012732>.
- [50] X.J. Zhao, G. Zhu, Y.J. Fan, H.Y. Li, Z.L. Wang, Triboelectric charging at the nanostructured solid/liquid interface for area-scalable wave energy conversion and its use in corrosion protection, *ACS Nano* 9 (7) (2015) 7671–7677. Available from: <https://doi.org/10.1021/acsnano.5b03093>.
- [51] L. Zong-Hong, C. Gang, W. Wenzhuo, P.K. C, W.Z. Lin, Dual-mode triboelectric nanogenerator for harvesting water energy and as a self-powered ethanol nanosensor, *ACS Nano* (2014) 6440–6448. Available from: <https://doi.org/10.1021/nn501983s>.
- [52] C. Gang, L. Zong-Hong, D. Zu-liang, W.Z. Lin, Simultaneously harvesting electrostatic and mechanical energies from flowing water by a hybridized triboelectric nanogenerator, *ACS Nano* (2014) 1932–1939. Available from: <https://doi.org/10.1021/nn406565k>.
- [53] S. Yuanjie, W. Xiaonan, Z. Guang, Y. Jin, C. Jun, B. Peng, et al., Hybrid triboelectric nanogenerator for harvesting water wave energy and as a self-powered distress signal emitter, *Nano Energy* (2014) 186–195. Available from: <https://doi.org/10.1016/j.nanoen.2014.07.006>.
- [54] Z. Xiaolong, Z. Youbin, W. Daoai, R.Z. Ur, Z. Feng, Liquid–solid contact triboelectrification and its use in self-powered nanosensor for detecting organics in water, *Nano Energy* (2016) 321–329. Available from: <https://doi.org/10.1016/j.nanoen.2016.10.025>.
- [55] L. Xiaoyi, T. Juan, Z. Jing, P. Caofeng, A nanowire based triboelectric nanogenerator for harvesting water wave energy and its applications, *APL Mater.* (2017) 074104. Available from: <https://doi.org/10.1063/1.4977216>.
- [56] S. Qiongfeng, W. Hao, W. Han, L. Chengkuo, Self-powered triboelectric nanogenerator buoy ball for applications ranging from environment monitoring to water wave energy farm, *Nano Energy* (2017) 203–213. Available from: <https://doi.org/10.1016/j.nanoen.2017.08.018>.
- [57] L. Pan, J. Wang, P. Wang, R. Gao, Y.C. Wang, X. Zhang, et al., Liquid-FEP-based U-tube triboelectric nanogenerator for harvesting water-wave energy, *Nano Res.* 11 (8) (2018) 4062–4073. Available from: <https://doi.org/10.1007/s12274-018-1989-9>.
- [58] X. Minyi, Z. Tiancong, W. Chuan, Z.S. L, L. Zhou, P. Xinxiang, et al., High power density tower-like triboelectric nanogenerator for harvesting arbitrary directional water wave energy, *ACS Nano* (2019). Available from: <https://doi.org/10.1021/acsnano.8b08274>.
- [59] X. Jiaqing, L. Meng-Fang, W. Jiangxin, G.S. Long, P. Kaushik, L.P. See, Wearable all-fabric-based triboelectric generator for water energy harvesting, *Adv. Energy Mater.* (2017) 1701243. Available from: <https://doi.org/10.1002/aenm.201701243>.
- [60] L. Xiaoyi, T. Juan, W. Xiandi, Z. Jing, P. Caofeng, W.Z. Lin, Networks of high performance triboelectric nanogenerators based on liquid-solid interface contact electrification for harvesting low-frequency blue energy, *Adv. Energy Mater.* (2018) 1800705. Available from: <https://doi.org/10.1002/aenm.201800705>.
- [61] N. Jinhui, W. Ziming, R. Zewei, L. Shuyao, C. Xiangyu, L.W. Zhong, Power generation from the interaction of a liquid droplet and a liquid membrane, *Nat. Commun.* (2019). Available from: <https://doi.org/10.1038/s41467-019-10232-x>.

- [62] B.D. Chen, W. Tang, C. He, C.R. Deng, L.J. Yang, L.P. Zhu, et al., Water wave energy harvesting and self-powered liquid-surface fluctuation sensing based on bionic-jellyfish triboelectric nanogenerator, *Mater. Today* 21 (1) (2018) 88–97. Available from: <https://doi.org/10.1016/j.mattod.2017.10.006>.
- [63] Y. Ya, Z. Hulin, L. Ruoyu, W. Xiaonan, H. Te-Chien, W.Z. Lin, Fully enclosed triboelectric nanogenerators for applications in water and harsh environments, *Adv. Energy Mater.* (2013) 1563–1568. Available from: <https://doi.org/10.1002/aenm.201300376>.
- [64] H. Youfan, Y. Jin, J. Qingshen, N. Simiao, W. Wenzhuo, W.Z. Lin, Triboelectric nanogenerator built on suspended 3D spiral structure as vibration and positioning sensor and wave energy harvester, *ACS Nano* (2013) 10424–10432. Available from: <https://doi.org/10.1021/nn405209u>.
- [65] W. Xiaonan, Y. Weiqing, J. Qingshen, W.Z. Lin, Harvesting broadband kinetic impact energy from mechanical triggering/vibration and water waves, *ACS Nano* (2014) 7405–7412. Available from: <https://doi.org/10.1021/nn502618f>.
- [66] L.M. Zhang, C.B. Han, T. Jiang, T. Zhou, X.H. Li, C. Zhang, et al., Multilayer wavy-structured robust triboelectric nanogenerator for harvesting water wave energy, *Nano Energy* 22 (2016) 87–94. Available from: <https://doi.org/10.1016/j.nanoen.2016.01.009>.
- [67] W.Z. Lin, Y. Jin, L. Zhaoling, F. Xing, Z. Yunlong, J. Qingshen, et al., Networks of triboelectric nanogenerators for harvesting water wave energy: a potential approach toward blue energy, *ACS Nano* (2015) 3324–3331. Available from: <https://doi.org/10.1021/acs.nano.5b00534>.
- [68] J. Qianwen, J. Yang, H. Yu, G. Caizhen, Z. Huarui, W. Magnus, et al., Self-powered electrochemical water treatment system for sterilization and algae removal using water wave energy, *Nano Energy* (2015) 81–88. Available from: <https://doi.org/10.1016/j.nanoen.2015.09.017>.
- [69] X. Liang, P. Yaokun, Z. Chi, J. Tao, C. Xiangyu, L. Jianjun, et al., Integrated triboelectric nanogenerator array based on air-driven membrane structures for water wave energy harvesting, *Nano Energy* (2017) 351–358. Available from: <https://doi.org/10.1016/j.nanoen.2016.11.037>.
- [70] J. Tao, Y. Yanyan, X. Liang, Z. Limin, X. Tianxiao, W.Z. Lin, Spring-assisted triboelectric nanogenerator for efficiently harvesting water wave energy, *Nano Energy* (2017) 560–567. Available from: <https://doi.org/10.1016/j.nanoen.2016.12.004>.
- [71] X.T. Xiao, J. Tao, Z.J. Xiong, L. Xi, X. Liang, S.J. Jia, et al., Silicone-based triboelectric nanogenerator for water wave energy harvesting, *ACS Appl. Mater. Interfaces* (2018) 3616–3623. Available from: <https://doi.org/10.1021/acsami.7b17239>.
- [72] T.X. Xiao, X. Liang, T. Jiang, L. Xu, J.J. Shao, J.H. Nie, et al., Spherical triboelectric nanogenerators based on spring-assisted multilayered structure for efficient water wave energy harvesting, *Adv. Funct. Mater.* 28 (35) (2018). Available from: <https://doi.org/10.1002/adfm.201802634>.
- [73] T. Jiang, L.M. Zhang, X. Chen, C.B. Han, W. Tang, C. Zhang, et al., Structural Optimization of Triboelectric Nanogenerator for Harvesting Water Wave Energy, *ACS Nano* 9 (12) (2015) 12562–12572. Available from: <https://doi.org/10.1021/acs.nano.5b06372>.
- [74] Y. Yanyan, J. Tao, Z. Limin, C. Xiangyu, G. Zhenliang, W.Z. Lin, Charging system optimization of triboelectric nanogenerator for water wave energy harvesting and storage, *ACS Appl. Mater. Interfaces* (2016) 21398–21406. Available from: <https://doi.org/10.1021/acsami.6b07697>.
- [75] Xu Liang, J. Tao, L. Pei, S.J. Jia, H. Chuan, Z. Wei, et al., Coupled triboelectric nanogenerator networks for efficient water wave energy harvesting, *ACS Nano* (2018) 1849–1858. Available from: <https://doi.org/10.1021/acs.nano.7b08674>.
- [76] W.Z. Lin, G. Hengyu, W. Zhen, Z. Chunlei, Y. Xing, L. Xinyuan, et al., Largely enhanced triboelectric nanogenerator for efficient harvesting of water wave energy by soft contacted structure, *Nano Energy* (2019) 432–439. Available from: <https://doi.org/10.1016/j.nanoen.2018.12.054>.

- [77] L. Wenbo, X. Liang, B. Tianzhao, Y. Hang, L. Guoxu, L. Wenjian, et al., Torus structured triboelectric nanogenerator array for water wave energy harvesting, *Nano Energy* (2019) 499–507. Available from: <https://doi.org/10.1016/j.nanoen.2019.01.088>.
- [78] X. Yang, L. Xu, P. Lin, W. Zhong, Y. Bai, J. Luo, et al., Macroscopic self-assembly network of encapsulated high-performance triboelectric nanogenerators for water wave energy harvesting, *Nano Energy* 60 (2019) 404–412. Available from: <https://doi.org/10.1016/j.nanoen.2019.03.054>.
- [79] L. Zhiming, Z. Binbin, G. Hengyu, W. Zhiyi, Z. Haiyang, Y. Jin, et al., Super-robust and frequency-multiplied triboelectric nanogenerator for efficient harvesting water and wind energy, *Nano Energy* (2019) 103908. Available from: <https://doi.org/10.1016/j.nanoen.2019.103908>.
- [80] W. Zhong, L. Xu, X. Yang, W. Tang, J. Shao, B. Chen, et al., Open-book-like triboelectric nanogenerators based on low-frequency roll-swing oscillators for wave energy harvesting, *Nanoscale* 11 (15) (2019) 7199–7208. Available from: <https://doi.org/10.1039/c8nr09978b>.
- [81] L. Rui, Z. Hua, N. Jinhui, Z. Wei, B. Yu, L. Xi, et al., Butterfly-inspired triboelectric nanogenerators with spring-assisted linkage structure for water wave energy harvesting, *Adv. Mater. Technol.* (2019) 1800514. Available from: <https://doi.org/10.1002/admt.201800514>.
- [82] C. Xiaoliang, X. Jiaqing, P. Kaushik, G. Meiling, W. Cheng, W. Chao, et al., Transparent and stretchable bimodal triboelectric nanogenerators with hierarchical micro-nanostructures for mechanical and water energy harvesting, *Nano Energy* (2019) 103904. Available from: <https://doi.org/10.1016/j.nanoen.2019.103904>.
- [83] L. Guanlin, G. Hengyu, X. Sixing, H. Chenguo, W.Z. Lin, Oblate spheroidal triboelectric nanogenerator for all-weather blue energy harvesting, *Adv. Energy Mater.* (2019) 1900801. Available from: <https://doi.org/10.1002/aenm.201900801>.
- [84] X. Liang, T. Jiang, G. Liu, Y. Feng, C. Zhang, Z.L. Wang, Spherical triboelectric nanogenerator integrated with power management module for harvesting multidirectional water wave energy, *Energy Environ. Sci.* 13 (1) (2020) 277–285. Available from: <https://doi.org/10.1039/c9ee03258d>.